Improving the conductance of carbon nanotube networks through resonant momentum exchange

Robert A. Bell,[1] Michael C. Payne,[1] and Arash A. Mostofi[2]
[1]*Theory of Condensed Matter Group, Cavendish Laboratory, Cambridge, UK*
[2]*Departments of Materials and Physics, and the Thomas Young Centre for Theory and Simulation of Materials, Imperial College London, London SW7 2AZ, UK*
(Received 22 December 2013; revised manuscript received 22 May 2014; published 18 June 2014)

We present a mechanism to improve the conductivity of carbon nanotube (CNT) networks by improving the conductance between CNTs of different chirality. We argue generally that a weak perturbation, e.g., from naturally present environmental impurities, can greatly improve the intertube conductance by allowing momentum-conserving tunneling. The mechanism is verified with a tight-binding model, and investigated for a network containing a range of chiralities. We conclude that improving the CNT purity by removing impurities may, counterintuitively, attenuate the overall network conductance.

DOI: 10.1103/PhysRevB.89.245426 PACS number(s): 73.63.Fg, 72.10.−d, 73.22.−f, 73.23.Ad

The remarkable electronic properties of single-walled carbon nanotubes (CNTs) make them excellent candidates for electronic devices of the future [1–5]. While there exist nanoscale applications that employ CNTs individually [1,6], considerable interest has focused on utilizing bulk CNT networks, with applications including macroscopic lightweight wires [4,7,8] and transparent conducting films [5,9].

Retaining the properties of individual CNTs when scaling up to the manufacture of these networks remains a significant challenge. For example, the conductivity of CNT wires is orders of magnitude lower than expected from the theoretical conductivity of individual CNTs [4,7,8,10]. In a macroscopic CNT network, no single CNT spans the two ends; to traverse the device, electrons must travel through pathways involving many CNTs. The overall conductivity of a CNT network, therefore, is determined not only by the intrinsic (intratube) conductivity of the individual CNTs, but also by the morphology of the network [11] and by the intertube conductivity.

One route to improving network conductivity, therefore, is to improve intertube tunneling. There have been several studies on intertube transport between the ends of capped or terminated CNTs [12–14]. The tendency for CNTs to align axially in bundles, however [15], together with their high aspect ratio, gives a relatively larger side-wall contact region over which intertube tunneling can be improved [16]. Side-wall intertube conduction between perfect CNTs has been shown to be strongly suppressed for CNTs of different chirality when compared to those of the same chirality [17,18]. This is a consequence of the sensitivity of CNT electronic structure to chirality and the requirement for both momentum and energy conservation in the tunneling process. Because typical synthesis methods generate CNT networks with a range of chiralities, the overall conductance of the CNT network may be strongly suppressed even if the constituent CNTs are defect free, perfectly aligned, and only metallic in character.

Improving side-wall conductance has proved difficult, because modifications that strongly interact with the CNTs, say through covalently bonded groups [19], defects [18], or adsorbed transition metal ions [16], dramatically reduce the intrinsic conductance of individual CNTs. Weak interactions with adsorbed molecules have been shown to improve side-wall tunneling [20], but this mechanism requires molecular states close in energy to the CNT Fermi energy and, therefore, the effectiveness of this approach is dependent on extrinsic factors that may be difficult to control.

In this paper we consider the general problem of electron transport between CNTs of arbitrary chirality. We focus on transport between metallic CNTs, but our conclusions equally apply to semiconducting ones and to bulk intersheet conduction in twisted bilayer graphene [21]. Our main result is that transport between tubes of different chirality can be greatly enhanced by the presence of a *weak* external potential that achieves momentum-conserving tunneling by enabling momentum exchange.

The fact that the potential need only be weak removes the need to modify the bonding structure of the CNTs and, hence, the intrinsic CNT conductance is unaffected. Furthermore, for a potential that varies on length scales larger than interatomic bond lengths, backscattering is forbidden and the total conductivity of the network is only improved by its presence. We conclude that interactions between the CNTs and environmental impurities likely accomplish this enhancement and that, counterintuitively, the presence of weak disorder in CNT networks is vital to ensuring a high network conductivity. Our analytical results are fully supported and verified by numerical tight-binding electron transport calculations.

We consider a system containing two metallic CNTs of arbitrary chirality axially aligned as shown schematically in Fig. 1. We denote the intrinsic tunneling interaction between the CNTs by the operator $\hat{H}_T$. Taking $|\psi_1\rangle$ and $|\psi_2\rangle$ to be electronic states at the Fermi energy E_F localized in each CNT, respectively, the contribution from these states to the small bias conductance $G_{1\to2}$ can be calculated using linear response theory. To first order,

$$G_{1\to2} = 2e^2\Gamma^{(1)}_{1\to2}\rho_1(E_\mathrm{F}), \tag{1}$$

$$\Gamma^{(1)}_{1\to2} = \frac{2\pi}{\hbar}\rho_2(E_\mathrm{F})|\langle\psi_1|\hat{H}_T|\psi_2\rangle|^2, \tag{2}$$

where $\Gamma^{(1)}_{1\to2}$ is the first-order tunneling rate between $|\psi_1\rangle$ and $|\psi_2\rangle$, and $\rho_1(E_\mathrm{F})$ and $\rho_2(E_\mathrm{F})$ are the densities of states at the Fermi level for the two CNTs. The most relevant term in Eq. (2) is the matrix element and its dependence on the momenta of the initial and final states and, in turn, on the chiralities of the two CNTs.

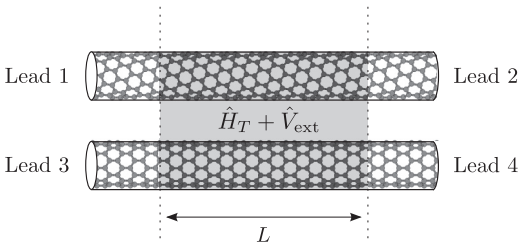

FIG. 1. The four-lead side-wall tunneling geometry considered in this work. The tunneling and external interaction occur in the shaded region, over a length scale L, outside of which the leads are isolated.

For CNT diameters typical to networks, the electronic states of the CNTs and their momenta are well described by the band structure of graphene under a zone- folding approximation [22]. For two weakly-interacting axially-aligned CNTs we may consider two graphene Brillouin zones, each rotated by the chiral angle of the respective CNTs such that their axial momenta are aligned [17], as shown schematically in Fig. 2.

Scattering between CNT states at the Fermi energy is equivalent to scattering between the Dirac points of these rotated Brillouin zones,[1] which in general have different momenta. This momentum difference, containing both axial and azimuthal components, increases as the difference in chiral angle increases.

For two CNTs that are commensurate (i.e., the ratio of the unit cell lengths is a rational fraction), the tunneling interaction is translationally invariant and momentum must be strictly conserved [17], resulting in the remarkable conclusion that conductance between pristine CNTs of different chirality is zero. The more common scenario, however, is that the CNTs are incommensurate, in which case translational invariance is broken [17,23], and the requirement for momentum conservation is no longer strict. Nonetheless, it has been shown that intertube conductance at first order is still strongly suppressed for CNTs of different chirality due to the momentum mismatch of initial and final states [17,23]. Irrespective of whether commensurate or not, therefore, there is a strong suppression of intertube transport between CNTs of mismatched chirality.

How may the intertube conductance between CNTs of different chirality be improved? There are two general statements that can be made about any additional tunneling interaction: (1) it must couple two states that are spatially separated and localized on different CNTs; (2) it must accept any momentum difference between the conducting states.

We consider the effect of an extrinsic *weak* local potential $V_{\rm ext}(\mathbf{r})$ (which may be thought of as arising from the interaction of the environment with the CNTs) and consider the conditions it must satisfy to improve intertube conductance. To improve conductance at first order, because the initial and final states are localized to different CNTs, $V_{\rm ext}$ would need to perturb the contact region between the CNTs where there is the greatest spatial overlap. While defects [18], functionalization [16], and structural deformations [18,24] may achieve

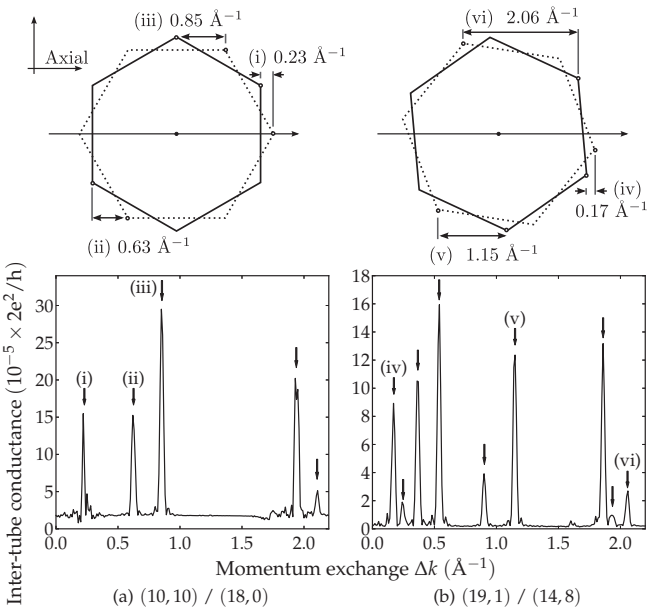

FIG. 2. Top: schematic representation of tunneling between CNTs. The hexagons represent the first graphene Brillouin zone (BZ) for CNT pairs: (a) (10,10)/(18,0) (dotted line/solid line) and (b) (19,1)/(14,8) (dotted/solid). Each BZ has been rotated so that the axial momentum lies along the horizontal. The metallic states are at the BZ corners. Bottom: corresponding momentum exchange dependence of intertube conductance at the Fermi level. Vertical arrows indicate the predicted momentum exchanges corresponding to scattering between Dirac points. For selected peaks, we show in the top panel the Dirac points involved in the scattering.

this, they may also significantly reduce the intrinsic intratube conductance [19,25] and, particularly in the case of side-wall functionalization, may increase the intertube separation and hence the tunneling barrier.

To circumvent these problems, we consider alternative mechanisms and examine the second-order scattering rate:

$$\Gamma^{(2)}_{1\to 2} = \frac{2\pi}{\hbar}\rho_2(E_{\rm F})\left|\sum_m \frac{\langle\psi_1|\hat{H}'_T|m\rangle\langle m|\hat{H}'_T|\psi_2\rangle}{E_{\rm F}-E_m}\right|^2, \quad (3)$$

where $\hat{H}'_T$ is the sum of the tunneling interaction and the extrinsic potential, $\hat{H}'_T = \hat{H}_T + V_{\rm ext}$, and the sum runs over all possible states $|m\rangle$. Expanding the matrix element gives four terms

$$\begin{aligned}\langle\psi_1|\hat{H}'_T|m\rangle\langle m|\hat{H}'_T|\psi_2\rangle &= \langle\psi_1|\hat{H}_T|m\rangle\langle m|\hat{H}_T|\psi_2\rangle + \langle\psi_1|\hat{H}_T|m\rangle\langle m|V_{\rm ext}|\psi_2\rangle \\ &\quad + \langle\psi_1|V_{\rm ext}|m\rangle\langle m|\hat{H}_T|\psi_2\rangle + \langle\psi_1|V_{\rm ext}|m\rangle\langle m|V_{\rm ext}|\psi_2\rangle. \end{aligned} \quad (4)$$

The first and final terms correspond to an even number of intertube scatterings and hence do not contribute to the intertube conductance. The remaining two terms, however, can be large if $V_{\rm ext}$ strongly couples states in the same CNT but with different momenta.

The third term, for example, represents scattering the initial state to an intermediate state $|m\rangle$ localized within the same

[1]In Ref. [17], Eqs. (2.11) and (2.12) apply to a general tunneling interaction thus proving this statement.

CNT possibly with different momentum, which then scatters into the other CNT. If V_{ext} is chosen such that the intermediate state has the same momentum as the final state, then intertube tunneling by $\hat{H}_T$ is no longer suppressed, and can be much larger than first-order tunneling.

We validate the above mechanism with numerical results using a tight binding model. The system Hamiltonian is given by

$$\hat{H} = \sum_{\alpha=1}^{2} \hat{H}_\alpha + \hat{H}_T + \hat{V}_{\text{ext}}, \tag{5}$$

where $\alpha = 1,2$ indexes the two CNTs. The band structures of the CNTs are described using a π-orbital model including nearest-neighbor hopping

$$\hat{H}_\alpha = -t_0 \sum_{\langle i,j \rangle} (c_{i\alpha}^\dagger c_{j\alpha} + c_{j\alpha}^\dagger c_{i\alpha}), \tag{6}$$

where $c_{i\alpha}^\dagger$ and $c_{i\alpha}$ are the creation and annihilation operators, respectively, for an electron on atomic site i, at position $\mathbf{r}_i$, belonging to CNT α. The summation is performed over nearest-neighbor sites $\langle i,j \rangle$ on a rolled hexagonal lattice, with interatomic bond lengths $a_{\text{C-C}} = 1.415$ Å. The Fermi energy is set to zero and the hopping parameter $t_0 = 2.77$ eV.

The intrinsic tunneling interaction between the CNTs is

$$\hat{H}_T = -\sum_{ij} t_{ij} (c_{i1}^\dagger c_{j2} + c_{j2}^\dagger c_{i1}), \tag{7}$$

where atom sites i, j are on different CNTs. Following Refs. [17] and [18], the tunneling matrix element is

$$t_{ij} = t_\perp e^{-|\mathbf{r}_i - \mathbf{r}_j|/\delta}, \tag{8}$$

with $t_\perp = 492$ eV and $\delta = 0.5$ Å. The separation between the surfaces of the CNTs is 3.4 Å.

For the external potential, we make the ansatz $V_{\text{ext}}(\mathbf{r}) = V_0 \sin(\Delta k z)$ (the z axis is chosen as the CNT axial direction), which scatters strongly between states in the same CNT with axial momenta differing by Δk. In the tight binding basis, this potential is approximated as diagonal

$$\hat{V}_{\text{ext}} = \sum_{i\alpha} V_0 \sin(\Delta k z_{i\alpha}) c_{i\alpha}^\dagger c_{i\alpha}, \tag{9}$$

and therefore does not directly couple the two CNTs. The amplitude $V_0 = 0.1$ eV (i.e., $V_0 \ll t_0$). A physical external potential can be considered as a sum of these Fourier components. We use a damping function to mutually isolate the leads with negligible contact-induced scattering [18]. Bulk intertube scattering occurs over a length $L = 190$ Å (Fig. 1).

The ballistic conductance between the four semi-infinite leads is calculated using the Landauer-Büttiker formalism via a Green's function approach [26]. We define the intertube conductance as the sum of the conductances between a lead and the two leads of the other CNT.

By ensuring that V_{ext} varies only on length scales greater than the interatomic bond length $a_{\text{C-C}}$, backscattering is vanishing [27], corresponding to a maximum momentum exchange presented in this work $\Delta k_{\max} = \pi / a_{\text{C-C}}$. We denote the resonant momentum exchanges and potentials as $\Delta k^\star$ and $V_{\text{ext}}(\Delta k^\star)$.

In Fig. 2 we plot for two CNT pairs the intertube conductance at the Fermi energy as a function of the momentum exchange Δk. The results are typical for CNT pairs with low intrinsic intertube conductance. We observe resonant peaks where the intertube conductance increases greatly. The momentum exchanges Δk correspond precisely to the axial momentum difference between Dirac points. We indicate these predicted positions with arrows and show for selected peaks (Fig. 2, top) the corresponding Dirac point scatterings.

The relative peak amplitudes are dependent on the form of the tight binding model and the spatial forms and energies of the intermediate states. Off momentum resonance, the intertube conductance is unaffected by the weak potential,

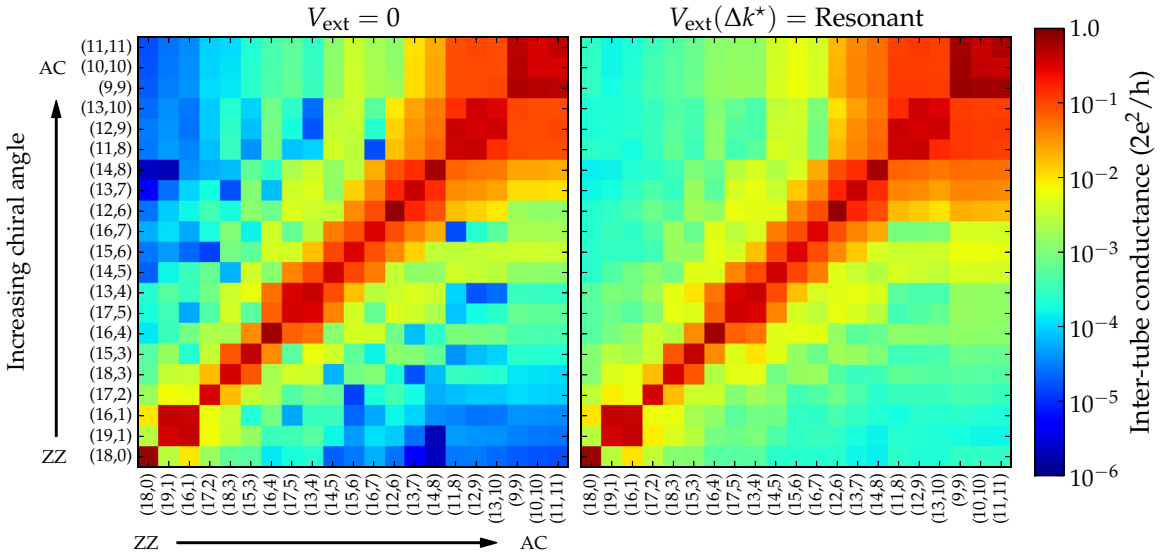

FIG. 3. (Color online) The intertube conductance between all pairs of metallic CNTs in the diameter range 1.2–1.6 nm. Left: intrinsic conductance $V_{\text{ext}} = 0$; right: maximum enhanced conductance (V_{ext} resonant). The CNTs are ordered by increasing chiral angle and labeled by the (n,m) chiral indices.

but for low momentum exchanges there is no decrease in the intratube conductance [28]. A similar momentum resonance occurs between pairs of semiconductor CNTs [28].

Realistic CNT networks are compositionally disordered in the sense that they contain CNTs with a range of chiralities. The left panel of Fig. 3 shows the intrinsic intertube conductance ($V_{\text{ext}} = 0$) at the Fermi energy between all pairs of metallic CNTs in the diameter range 1.2–1.6 nm. Where both CNTs are chiral, we show the conductance only for CNTs of opposite handedness; quantitatively equivalent results are obtained for pairs of CNTs of the same handedness [28]. The CNTs are ordered by increasing chiral angle. From the peak along the diagonal, it is evident that intertube conductance is large between CNTs of the same or similar chirality. As the difference in chirality between two CNTs increases, however, momentum-conserving tunneling is not possible and intertube conductance is strongly suppressed.

The right panel of Fig. 3 shows the intertube conductance on the addition of the momentum-resonant potential $V_{\text{ext}}(\Delta k^\star)$, at which the intertube conductance is a maximum. The conductance between CNTs of the same chirality is unaffected and remains high, while there is a strong enhancement for CNTs of different chirality.

For different CNT pairs the intertube conductance is maximized by different momentum exchanges $\Delta k^\star$ (see, e.g., Fig. 2), which are found to be distributed uniformly across a broad range of momentum [28]. The external potential, therefore, should contain a wide range of resonant momenta to improve the conductance of a network consisting of a wide range of CNT chiralities. The Fourier components of this potential that provide resonant momentum-exchange will automatically improve the intertube conductance, and there is no need to fine tune the external potential.

Finally, we consider this mechanism at energies away from the Fermi level. As a result of the linear dispersion relations around the Dirac points, for states traveling in the same direction the momentum exchange is resonant over a wide band of energies around the Fermi level. This is shown in Fig. 4 where we plot the transmission spectrum between leads 1 and 4. (Transmission between leads 1 and 3 is resonant at the Fermi energy only [28].) This mechanism is therefore insensitive to the small band gap in non-armchair metallic CNTs [29] and applies to doped CNT networks.

To summarize our results, we present a mechanism to improve the side-wall intertube conductance between CNTs of different chirality. We find that while the best method is to reduce the range of chiralities present, significant improvements can be made with a weak external potential allowing momentum exchange with the environment, promoting momentum-conserving scattering.

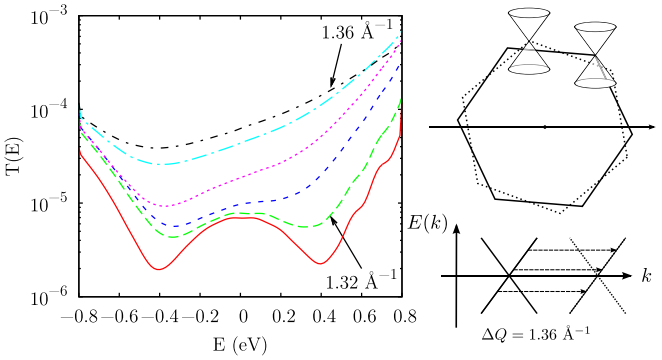

FIG. 4. (Color online) Left: the transmission between leads 1 and 4 for the (12,9)/(13,4) CNT pair as a function of electron energy for $\hat{V}_{\text{ext}} = 0$ (solid red), and for momentum transfer increasing in steps of 0.01 Å^{-1} from $\Delta k = 1.32$ Å^{-1} (dashed green) to $\Delta k = 1.36$ Å^{-1} (dot-dashed black) where momentum resonance occurs. Transmission increases as resonance is approached. The Fermi energy is zero. Right: the Dirac points involved in this resonance, and the projection of the dispersion relation onto the axial momentum axis. The momentum exchange, indicated by the arrows, is resonant over a wide range of energies around the Fermi level.

By ensuring that the potential varies slowly compared to the interatomic distance, backscattering is vanishing [27], and as the mechanism is second order, the perturbation can be localized away from the contact region. Chemical bonding is not required, and instead weaker, long-range physical interactions can be utilized. Possible candidates include electrostatic influences of adsorbed molecules; substrate surface reconstructions; Moiré patterns induced in multiwalled CNTs [30]; phonon-assisted tunneling; and polymer-wrapped CNTs [31]. Indeed, enhancements caused by this mechanism are likely already present in the material due to naturally-occurring disorder. Improving the quality of the material by removing this disorder may counterintuitively reduce the conductance of these CNT networks.

The authors thank S. Dubois for his implementation for calculating transmission spectra. R.A.B. acknowledges financial support from British Telecommunications and an EPSRC studentship. Calculations were performed using the the Darwin Supercomputer of the University of Cambridge High Performance Computing Service.

[1] M. M. Shulaker, G. Hills, N. Patil, H. Wei, H.-Y. Chen, H.-S. P. Wong, and S. Mitra, Nature **501**, 526 (2013).
[2] Q. Cao and S.-j. Han, Nanoscale **5**, 8852 (2013).
[3] J. Appenzeller, Proc. IEEE **96**, 201 (2008).
[4] N. Behabtu, M. J. Green, and M. Pasquali, Nano Today **3**, 24 (2008).
[5] Q. Cao and J. A. Rogers, Adv. Mater. **21**, 29 (2009).
[6] A. D. Franklin, M. Luisier, S.-J. Han, G. Tulevski, C. M. Breslin, L. Gignac, M. S. Lundstrom, and W. Haensch, Nano Lett. **12**, 758 (2012).
[7] R. M. Sundaram, K. K. K. Koziol, and A. H. Windle, Adv. Mater. **23**, 5064 (2011).
[8] N. Behabtu, C. C. Young, D. E. Tsentalovich, O. Kleinerman, X. Wang, A. W. K. Ma, E. A. Bengio, R. F. ter Waarbeek, J. J. de Jong, R. E. Hoogerwerf *et al.*, Science **339**, 182 (2013).

[9] Z. Wu, Z. Chen, X. Du, J. M. Logan, J. Sippel, M. Nikolou, K. Kamaras, J. R. Reynolds, D. B. Tanner, A. F. Hebard *et al.*, Science **305**, 1273 (2004).
[10] J. Alvarenga, P. R. Jarosz, C. M. Schauerman, B. T. Moses, B. J. Landi, C. D. Cress, and R. P. Raffaelle, Appl. Phys. Lett. **97**, 182106 (2010).
[11] L. Hu, D. S. Hecht, and G. Grüner, Nano Lett. **4**, 2513 (2004).
[12] S.-H. Ke, H. U. Baranger, and W. Yang, Phys. Rev. Lett. **99**, 146802 (2007).
[13] Z. Qian, S. Hou, J. Ning, R. Li, Z. Shen, X. Zhao, and Z. Xue, J. Chem. Phys. **126**, 084705 (2007).
[14] T. B. Martins, A. Fazzio, and A. J. R. da Silva, Phys. Rev. B **79**, 115413 (2009).
[15] M. Ge and K. Sattler, Appl. Phys. Lett. **64**, 710 (1994).
[16] E. Y. Li and N. Marzari, ACS Nano **5**, 9726 (2011).
[17] A. A. Maarouf, C. L. Kane, and E. J. Mele, Phys. Rev. B **61**, 11156 (2000).
[18] M. A. Tunney and N. R. Cooper, Phys. Rev. B **74**, 075406 (2006).
[19] Y.-S. Lee, M. B. Nardelli, and N. Marzari, Phys. Rev. Lett. **95**, 076804 (2005).
[20] D. J. Mowbray, C. Morgan, and K. S. Thygesen, Phys. Rev. B **79**, 195431 (2009).
[21] T. Ohta, J. T. Robinson, P. J. Feibelman, A. Bostwick, E. Rotenberg, and T. E. Beechem, Phys. Rev. Lett. **109**, 186807 (2012).
[22] J.-C. Charlier, X. Blase, and S. Roche, Rev. Mod. Phys. **79**, 677 (2007).
[23] Y.-G. Yoon, P. Delaney, and S. G. Louie, Phys. Rev. B **66**, 073407 (2002).
[24] Y.-G. Yoon, M. S. C. Mazzoni, H. J. Choi, J. Ihm, and S. G. Louie, Phys. Rev. Lett. **86**, 688 (2001).
[25] H. J. Choi, J. Ihm, S. G. Louie, and M. L. Cohen, Phys. Rev. Lett. **84**, 2917 (2000).
[26] S. Datta, *Electronic Transport in Mesoscopic Systems* (Cambridge University, Cambridge, England,1995).
[27] T. Ando and T. Nakanishi, J. Phys. Soc. Jpn. **67**, 1704 (1998).
[28] See Supplemental Material at http://link.aps.org/supplemental/10.1103/PhysRevB.89.245426 for the details of additional calculations discussed in the main text.
[29] C. L. Kane and E. J. Mele, Phys. Rev. Lett. **78**, 1932 (1997).
[30] N. Fukui, Y. Suwa, H. Yoshida, T. Sugai, S. Heike, M. Fujimori, Y. Terada, T. Hashizume, and H. Shinohara, Phys. Rev. B **79**, 125402 (2009).
[31] Y. Ma, W. Cheung, D. Wei, A. Bogozi, P. L. Chiu, L. Wang, F. Pontoriero, R. Mendelsohn, and H. He, ACS Nano **2**, 1197 (2008).